
Mortar coupling of multiphase flow and reactive transport on non-matching grids

Mary F. Wheeler* — Gergina Pencheva** — Sunil G. Thomas**

* *Institute for Computational Engineering and Sciences,
Department of Aerospace Engineering & Engineering Mechanics,
and Department of Petroleum and Geosystems Engineering,
The University of Texas at Austin,
Austin, TX 78712*

mfw@ices.utexas.edu

** *Institute for Computational Engineering and Sciences,
The University of Texas at Austin,
Austin, TX 78712*

{gergina, sgthomas}@ices.utexas.edu

ABSTRACT. We formulate a cell-volume method (expanded MFEM) for coupling multiphase flow and reactive transport in porous media. Multiphase flow is modeled using mortar mixed finite elements that allows for accurate and efficient parallel domain decomposition with non-matching grids. The reactive transport equations are treated using operator splitting for decoupling transport and reactions. Computational results are presented. Theoretical results are not provided owing to space restrictions.

KEYWORDS: cell volume, mortar, mixed FEM, operator splitting, advection, diffusion, reaction

1. Introduction

Microbial bio-degradation plays an important role in rendering subsurface contaminants harmless. It is a naturally occurring process that can be accelerated to protect potable water supply. Modeling this complex process is computationally challenging. It involves both flow and transport that occur over varying spatial and temporal scales. The transport is often characterized by advection, reaction and diffusion. The reaction stage involves chemical interaction between hydrocarbons, microbes, oxygen, nitrogen and various other compounds. Therefore, simple and efficient numerical methods are desirable in the simulation of these processes which is of critical importance in designing adequate bio-restoration mechanisms.

2. Flow in porous media

We consider time-dependent two-phase immiscible flow in porous media on a domain Ω , decomposed into non-overlapping subdomain blocks Ω_i so that $\bar{\Omega} = \cup_{i=1}^{n_b} \bar{\Omega}_i$. The blocks need not form a conforming partition. Let $\Gamma_{i,j} = \partial\Omega_i \cap \partial\Omega_j$, $\Gamma = \cup_{1 \leq i < j \leq n_b} \Gamma_{i,j}$, and $\Gamma_i = \partial\Omega_i \cap \Gamma = \partial\Omega_i \setminus \partial\Omega$. On Ω_i the governing mass balance and Darcy velocity equations [CHA 86] are:

$$\frac{\partial(\phi\rho_\alpha S_\alpha)}{\partial t} + \nabla \cdot (\rho_\alpha \mathbf{u}_\alpha) = q_\alpha, \quad [1]$$

$$\mathbf{u}_\alpha = -\frac{k_{r\alpha}(S_\alpha)K}{\mu_\alpha}(\nabla p_\alpha - \rho_\alpha g \nabla D), \quad [2]$$

where $\alpha = w$ (wetting), n (non-wetting) denotes the phase, \mathbf{u}_α , p_α , S_α , $\rho_\alpha(p_\alpha)$, $k_{r\alpha}(S_\alpha)$, μ_α , q_α are the phase velocity, pressure, saturation, density, relative permeability, viscosity, and source term, resp.; ϕ is the porosity, K is the rock permeability tensor, g is the gravitational constant, and D is the depth. For the case of one flowing phase, $S_\alpha \equiv 1$. On each $\Gamma_{i,j}$ meaningful continuity conditions are imposed, i.e., $p_\alpha|_{\Omega_i} = p_\alpha|_{\Omega_j}$, $[\mathbf{u}_\alpha \cdot \mathbf{n}]_{i,j} \equiv \mathbf{u}_\alpha|_{\Omega_i} \cdot \mathbf{n}_i + \mathbf{u}_\alpha|_{\Omega_j} \cdot \mathbf{n}_j = 0$. Further, saturation and capillary pressure constraints, $S_w + S_n = 1$, $p_c(S_w) = p_n - p_w$, are imposed. We assume that no flow $\mathbf{u}_\alpha \cdot \mathbf{n} = 0$ is imposed on $\partial\Omega$, although more general types of boundary conditions can also be treated. Two of the unknowns in [1]–[2] can be eliminated using these constraints. A common practice is to choose as primary variables one pressure and one saturation which we denote by p and S .

Let $\mathcal{T}_{h,i}$ be a conforming, quasi-uniform affine finite element partition of Ω_i , $1 \leq i \leq n_b$, of maximal element diameter h_i . Let $h = \max_{1 \leq i \leq n_b} h_i$. Note that we allow for the possibility that the subdomain partitions $\mathcal{T}_{h,i}$ and $\mathcal{T}_{h,j}$ need not align on $\Gamma_{i,j}$. Define $\mathcal{T}_h = \cup_{i=1}^{n_b} \mathcal{T}_{h,i}$. Let $\mathbf{V}_{h,i} \times W_{h,i} \subset H(\text{div}; \Omega_i) \times L^2(\Omega_i)$ be any of the usual mixed finite element spaces defined on $\mathcal{T}_{h,i}$ (see [BRE 91], Section III.3). The most commonly used mixed spaces are the Raviart-Thomas spaces of order k , RT_k [RAV 77, NED 80]. Our simulator uses RT_0 space defined on a rectangular partition $\mathcal{T}_{h,i}$ by

$$\mathbf{V}_{h,i} = \{ \mathbf{v} : \forall E, F \in \mathcal{T}_{h,i}, (\alpha_1 x_1 + \beta_1, \alpha_2 x_2 + \beta_2, \alpha_3 x_3 + \beta_3)^T, \alpha_l, \beta_l \in \mathbb{R}, \\ \mathbf{v} \cdot \mathbf{n} \text{ is continuous across element faces and } \mathbf{v} \cdot \mathbf{n}_i = 0 \text{ on } \partial\Omega_i \cap \partial\Omega \},$$

$$W_{h,i} = \{ w : \forall E \in \mathcal{T}_{h,i}, w|_E = \alpha, \alpha \in \mathbb{R} \}.$$

Let $\mathcal{T}_{H,i,j}$ be a non-degenerate, quasi-uniform finite element partition of $\Gamma_{i,j}$ with maximal element diameter $H_{i,j}$, $\mathcal{T}^{\Gamma,H} = \cup_{1 \leq i < j \leq n_b} \mathcal{T}_{H,i,j}$, $H = \max_{1 \leq i, j \leq n_b} H_{i,j}$, and $M_{H,i,j} \subset L^2(\Gamma_{i,j})$ be the mortar space on $\Gamma_{i,j}$, containing at least either the continuous or discontinuous piecewise linears on $\mathcal{T}_{H,i,j}$. The velocity, pressure and mortar mixed finite element spaces are defined as follows:

$$\mathbf{V}_h = \bigoplus_{i=1}^{n_b} \mathbf{V}_{h,i}, \quad W_h = \bigoplus_{i=1}^{n_b} W_{h,i}, \quad M_H = \bigoplus_{1 \leq i < j \leq n_b} M_{H,i,j}.$$

Using the expanded mixed finite element method (ExpMFEM) [ARB 97], we let $\tilde{\mathbf{u}}_\alpha = -\nabla p_\alpha$; then $\mathbf{u}_\alpha = k_{r\alpha}(S_\alpha)K/\mu_\alpha(\tilde{\mathbf{u}}_\alpha + \rho_\alpha g \nabla D)$. The gradient $\tilde{\mathbf{u}}_\alpha$ is discretized in the space $\tilde{\mathbf{V}}_{h,i}$, which is the space $\mathbf{V}_{h,i}$ without imposing the no-flow boundary condition. This choice, with appropriate quadrature rules, eliminates $\tilde{\mathbf{u}}_\alpha$ and \mathbf{u}_α , reducing the method to cell-centered finite differences for the subdomain primary variables p_h and S_h , coupled with the mortar primary variables p_H and S_H , see [ARB 97] for details.

Let $0 = t_0 < t_1 < t_2 < \dots$, let $\Delta t^n = t_n - t_{n-1}$, and let $f^n = f(t_n)$, $\Delta f^n = f(t_n) - f(t_{n-1})$. In the backward Euler multiblock ExpMFEM for [1]-[2] we seek, for $1 \leq i < j \leq n_b$ and $n = 1, 2, 3, \dots$, $\mathbf{u}_{\alpha,h}^n|_{\Omega_i} \in \mathbf{V}_{h,i}$, $\tilde{\mathbf{u}}_{\alpha,h}^n|_{\Omega_i} \in \tilde{\mathbf{V}}_{h,i}$, $p_h^n|_{\Omega_i} \in W_{h,i}$, $S_h^n|_{\Omega_i} \in W_{h,i}$, $p_H^n|_{\Gamma_{i,j}} \in M_{H,i,j}$, and $S_H^n|_{\Gamma_{i,j}} \in M_{H,i,j}$ such that, for $\alpha = w$ and n ,

$$\left(\frac{\Delta(\varphi \rho_{\alpha,h} S_{\alpha,h})^n}{\Delta t^n}, w \right)_{\Omega_i} + (\nabla \cdot \rho_{\alpha,h}^n \mathbf{u}_{\alpha,h}^n, w)_{\Omega_i} = \left(q_\alpha^{n-\frac{1}{2}}, w \right)_{\Omega_i}, \quad w \in W_{h,i}, \quad [3]$$

$$(\tilde{\mathbf{u}}_{\alpha,h}^n, \mathbf{v})_{\Omega_i} = (p_{\alpha,h}^n, \nabla \cdot \mathbf{v})_{\Omega_i} - \langle p_{\alpha,H}^n, \mathbf{v} \cdot \mathbf{n}_i \rangle_{\Gamma_i}, \quad \mathbf{v} \in \mathbf{V}_{h,i}, \quad [4]$$

$$(\mathbf{u}_{\alpha,h}^n, \tilde{\mathbf{v}})_{\Omega_i} = \left(\frac{k_{r\alpha,h}^n \mathbf{K}}{\mu_{\alpha,h}} [\tilde{\mathbf{u}}_{\alpha,h}^n + \rho_{\alpha,h}^n g \nabla D], \tilde{\mathbf{v}} \right)_{\Omega_i}, \quad \tilde{\mathbf{v}} \in \tilde{\mathbf{V}}_{h,i}, \quad [5]$$

$$\langle [\mathbf{u}_{\alpha,h}^n \cdot \mathbf{n}]_{i,j}, \zeta \rangle_{\Gamma_{i,j}} = 0, \quad \zeta \in M_{H,i,j}. \quad [6]$$

2.1. Domain decomposition

Let $\mathbf{M}_H = M_H \times M_H$ be the space of mortar primary variables. Then define a non-linear interface bi-variate form $b^n : \mathbf{M}_H \times \mathbf{M}_H \rightarrow \mathbb{R}$ as follows. For $\psi = (p_{w,H}^n, S_{w,H}^n) \in \mathbf{M}_H$ and $\eta = (\eta_w, \eta_w) \in \mathbf{M}_H$ (where the mortar primaries are chosen to be water phase pressure and saturation); let

$$b^n(\psi, \eta) = \sum_{1 \leq i < j \leq n_b} \int_{\Gamma_{i,j}} \left([\rho_{w,h}^n \mathbf{u}_{w,h}^n(\psi) \cdot \mathbf{n}]_{ij} \eta_w + [\rho_{n,h}^n \mathbf{u}_{n,h}^n(\psi) \cdot \mathbf{n}]_{ij} \eta_n \right) ds,$$

where $\mathbf{u}_{\alpha,h}^n$ is obtained from the solution to the sub-domain problems using mixed finite elements, given in equations [3]–[6], with Dirichlet boundary data $p_{\alpha,H}^n(\psi)$.

Define a non-linear interface operator $\mathcal{B}^n : \mathbf{M}_H \rightarrow \mathbf{M}_H$ by

$$\langle \mathcal{B}^n \psi, \eta \rangle = b^n(\psi, \eta), \quad \forall \eta \in \mathbf{M}_H,$$

where $\langle \cdot, \cdot \rangle$ is the L^2 inner product in \mathbf{M}_H . It can be checked that $(\psi, p_{\alpha,h}^n(\psi), S_{\alpha,h}^n(\psi), \mathbf{u}_{\alpha,h}^n(\psi))$ solves the system [3]–[6] when $\psi \in \mathbf{M}_H$ is the solution of

$$\mathcal{B}^n(\psi) = 0. \quad [7]$$

The system of non-linear *interface* equations [7] is solved by an inexact Newton method. Each Newton step s is computed by a forward difference GMRES iteration

for solving $(\mathcal{B}^n)'(\psi)s = -\mathcal{B}^n(\psi)$. On each GMRES iteration, the action of the Jacobian $(\mathcal{B}^n)'(\psi)$ on a vector, η , is approximated by a forward difference approximation. Hence, it requires only one additional evaluation of the operator \mathcal{B}^n . See [YOT 01] for more details.

3. The reactive transport problem

Consider the reactive transport problem described by

$$\frac{\partial(\varphi c_{i\alpha} S_\alpha)}{\partial t} + \nabla \cdot (c_{i\alpha} \mathbf{u}_\alpha - \varphi S_\alpha \mathbf{D}_{i\alpha} \nabla c_{i\alpha}) = r(c_{i\alpha}), \quad [8]$$

$$\mathbf{D}_{i\alpha} \nabla c_{i\alpha} \cdot \mathbf{n} = 0, \quad [9]$$

where $\mathbf{D}_{i\alpha} = \mathbf{D}_{i\alpha}^{\text{diff}} + \mathbf{D}_{i\alpha}^{\text{hyd}}$ is the sum of *molecular diffusion* and *hydrodynamic dispersion*, $\mathbf{D}_{i\alpha}^{\text{diff}} = \tau_\alpha d_{m,i\alpha} \mathbf{I}$, $\varphi S_\alpha \mathbf{D}_{i\alpha}^{\text{hyd}} = d_{t,\alpha} |\mathbf{u}_\alpha| \mathbf{I} + (d_{l,\alpha} - d_{t,\alpha}) / |\mathbf{u}_\alpha| \mathbf{u}_\alpha \mathbf{u}_\alpha^T$. Here τ_α is the ‘‘tortuosity’’ of flow of phase α , $d_{m,i\alpha}$, $d_{l,\alpha}$, $d_{t,\alpha}$ are the *molecular diffusion*, *longitudinal*, and *transverse dispersion coefficients*, resp. The source takes the general form, $r(c_{i\alpha}) = r_{i\alpha}^I + \varphi S_\alpha r_{i\alpha}^C + q_{i\alpha}$ where the terms $r_{i\alpha}^I$ and $r_{i\alpha}^C$ model the influx (or efflux) from other phases and the chemical rate of decay (or formation) of species i in phase α , resp. The term $q_{i\alpha}$ models a source (or sink) for species i in phase α . Further, note that the net interchange of species between phases is zero; i.e., $\sum_\alpha r_{i\alpha} + r_{iR} = 0$. Here, r_{iR} is the influx (efflux) of species i into the stationary phases (for e.g., the rock matrix). For simplicity, assume there is no adsorption, hence $r_{iR} \equiv 0$.

3.1. A time-split scheme

We present a ‘‘phase-summed’’ formulation of [8]–[9]. An equilibrium partitioning of the species among the phases is assumed, given by constants $\theta_{i\alpha}$ so that $c_{i\alpha} = \theta_{i\alpha} c_{i\alpha_0}$, where α_0 is a reference phase, say, the water phase. Then summing the equations [8] and [9] over α , for a given species i , reduces it to,

$$\frac{\partial(\varphi_i^* c_{iw})}{\partial t} + \nabla \cdot (c_{iw} \mathbf{u}_i^* - \mathbf{D}_i^* \nabla c_{iw}) = r^*(c_{iw}), \quad [10]$$

$$\mathbf{D}_{iw} \nabla c_{iw} \cdot \mathbf{n} = 0. \quad [11]$$

The phase-summed asterisked (*) terms are defined as follows: $\varphi_i^* = \varphi \sum_\alpha \theta_{i\alpha} S_\alpha$, $\mathbf{u}_i^* = \sum_\alpha \theta_{i\alpha} \mathbf{u}_\alpha$, $\mathbf{D}_i^* = \varphi \sum_\alpha S_\alpha \theta_{i\alpha} \mathbf{D}_{i\alpha}$, $r^*(c_{iw}) = \varphi \sum_\alpha r_{i\alpha}^C + r_{iR} + \sum_\alpha q_{i\alpha}$.

Assume that at time $t = \tau_m$, the concentrations of all species are known. Assume also that $(\tau_m, \tau_{m+1}) \subset (t_n, t_{n+1})$ and that the values of \mathbf{u}_i^* and φ_i^* are known at the old and new flow time-steps, i.e., t_n and t_{n+1} . A direct discretization of the equation [10] yields,

$$\frac{T_i^{m+1} - T_i^m}{\Delta \tau^{m+1}} + \nabla \cdot (c_{iw}^m \mathbf{u}_i^{*,m+1/2} - \mathbf{D}_i^{*,m} \nabla c_{iw}^{m+1}) = r^*(c_{iw}^{m+1/2}). \quad [12]$$

Here, $\Delta\tau^{m+1} = \tau_{m+1} - \tau_m$ and $T_i = \varphi_i^* c_{iw}$. Note also that φ_i^* and \mathbf{u}_i^* are evaluated at time $t \in (\tau_m, \tau_{m+1})$ by linear interpolation between the known values at t_n and t_{n+1} . Direct solution of equation [12] is impractical. Hence, a time-split algorithm is employed in which the advection, chemical reaction and diffusion-dispersion components are solved “independently” of each other. Each component delivers intermediate values for T_i , labelled \bar{T}_i , \hat{T}_i and T_i^{m+1} . The individual steps of this algorithm are described below.

3.2. Advection

Let the true and approximate solution spaces for species concentration be the same as those defined for pressure (or saturation) defined in Section 2. The advection step is then given for $1 \leq j \leq n$ by

$$\left(\frac{\partial \varphi_i^* c_{iw}}{\partial t}, w \right)_{\Omega_j} + (\nabla \cdot (c_{iw} \mathbf{u}_i^*), w)_{\Omega_j} = \left(\sum_{\alpha} q_{i\alpha}, w \right)_{\Omega_j} \quad w \in W_j. \quad [13]$$

Equation [13] is solved by applying a first order Godunov scheme using upstream weighted concentrations. This eliminates any instability in the solution owing to the convection term, $\nabla \cdot (c_{iw} \mathbf{u}_i^*)$ that is known [CHA 84] to introduce spatial oscillations. Setting $T_i^m = \varphi_i^{*,m} c_{h,iw}^m$, an explicit in time approximation of the time derivative in [13] yields the weak form,

$$\left(\frac{\bar{T}_i - T_i^m}{\Delta\tau^{m+1}}, w \right)_{\Omega_j} + \sum_{E \in \mathcal{T}_{h,j}} \langle c_{h,iw}^{m,\text{upw}} \mathbf{u}_{h,i}^{*,m+1/2} \cdot \mathbf{n}_E, w \rangle_{\partial E} = \left(\sum_{\alpha} q_{i\alpha}, w \right)_{\Omega_j}, \quad w \in W_{h,j}$$

for \bar{T}_i from which the intermediate value of concentration, $\bar{c}_{h,iw}$ can be calculated using $\bar{c}_{h,iw} = \bar{T}_i / \varphi_i^{*,m+1}$.

3.3. Chemical Reaction

After the advection step is completed, we solve the chemical reaction component of [12] given by

$$\frac{\partial \varphi_i^* c_{iw}}{\partial t} = \varphi \sum_{\alpha} r_{i\alpha}^C \quad [14]$$

Explicit ODE integration can be used to solve [14], even exactly in some cases (depending on the right hand side). Approximations can be obtained by numerical integration; for e.g., with the first order forward-Euler scheme, [14] reduces to

$$\frac{\hat{T}_i - \bar{T}_i}{\Delta\tau^{m+1}} = \varphi \sum_{\alpha} r_{i\alpha}^C$$

For more accurate approximations, higher-order Runge-Kutta integration schemes are used in our simulator. For details on reaction laws, see [PES 01].

3.4. Diffusion-Dispersion

Next, we solve the diffusion-dispersion equation. This takes the form,

$$\frac{\partial(\varphi_i^* c_{iw})}{\partial t} - \nabla \cdot \mathbf{D}_i^* \nabla c_{iw} = 0. \quad [15]$$

This is solved fully implicitly using ExpMFEM with the full-tensor \mathbf{D}_i^* as discussed in Section 2. In the discretized weak form of [15], introducing $\tilde{\mathbf{z}} = -\nabla c$ and $\mathbf{z} = \mathbf{D}_i^* \tilde{\mathbf{z}}$, an ExpMFEM seeks $\tilde{\mathbf{z}}_{h,iw}^{m+1}|_{\Omega_j} \in \tilde{\mathbf{V}}_{h,j}$, $\mathbf{z}_{h,iw}^{m+1}|_{\Omega_j} \in \mathbf{V}_{h,j}$, $c_{h,iw}^{m+1}|_{\Omega_j} \in W_{h,j}$, such that, for $1 \leq j \leq n_b$,

$$\left(\frac{\varphi_i^{*,m+1} c_{h,iw}^{m+1} - \varphi_i^{*,m} c_{h,iw}^m}{\Delta \tau^{m+1}}, w \right)_{\Omega_j} + \left(\nabla \cdot \mathbf{z}_{h,iw}^{m+1}, w \right)_{\Omega_j} = 0, \quad w \in W_{h,j}, \quad [16]$$

$$(\tilde{\mathbf{z}}_{h,iw}^{m+1}, \mathbf{v})_{\Omega_j} = (c_{h,iw}^{m+1}, \nabla \cdot \mathbf{v})_{\Omega_j} - \langle \mathcal{P}_j c_{h,iw}, \mathbf{v} \cdot \mathbf{n}_j \rangle_{\Gamma_j}, \quad \mathbf{v} \in \mathbf{V}_{h,j}, \quad [17]$$

$$(\mathbf{z}_{h,iw}^{m+1}, \tilde{\mathbf{v}})_{\Omega_j} = (\mathbf{D}_i^{*,m+1} \tilde{\mathbf{z}}_{h,iw}^{m+1}, \tilde{\mathbf{v}})_{\Omega_j}, \quad \tilde{\mathbf{v}} \in \tilde{\mathbf{V}}_{h,i}. \quad [18]$$

Here, $\mathcal{P}_j : L^2(\Gamma_j) \rightarrow L^2(\Gamma_k)$ is an L^2 -orthogonal projection satisfying $\forall \phi \in L^2(\Gamma_j)$

$$\langle \phi - \mathcal{P}_j \phi, \mathbf{v} \cdot \mathbf{n}_j \rangle_{\Gamma_{k,j}} = 0, \quad \forall \mathbf{v} \in \mathbf{V}_{h,i}, \forall k \text{ such that } \bar{\Omega}_k \cap \bar{\Omega}_j \neq \emptyset.$$

Following [ARB 97], suitable quadrature rules can be defined to approximate the integrals appearing in [16]–[18], thereby eliminating $\tilde{\mathbf{z}}_{h,iw}$ and $\mathbf{z}_{h,iw}$ in terms of $c_{h,iw}$.

4. Numerical experiments

Here, we present a NAPL remediation example. A square-shaped domain is considered with dimensions 20 ft \times 400 ft \times 400 ft. The permeability and flow field (superimposed on tracer profile for a multiblock case) are shown in figure 1. The two

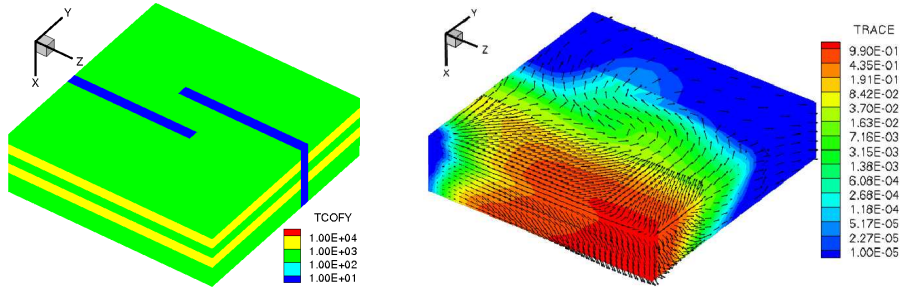


Figure 1. Permeability and flow fields for NAPL remediation problem.

barriers obstructing the flow render it challenging for coupled flow and transport. The

species interacting in this problem are NAPL (toluene), dissolved O_2 , N_2 , microbes, bio-degraded products (water and carbon dioxide) and a non-radioactive tracer. There are two wells arranged in a quarter-five spot pattern that inject water and produce oil. No-flow and zero diffusive flux boundary conditions are assumed in this problem.

At initial time, the tracer, toluene and the microbes occupy a thin strip on the left-end of the domain, i.e., $0 \leq y \leq 40'$ in figure 1 while O_2 and N_2 occupy the rest of the domain $40' \leq y \leq 400'$. The microbial kinetics and other reactions occurring in this system are governed by equations presented in [PES 01]. The problem is solved first assuming a single-domain with a fine ($10 \times 40 \times 40$) grid.

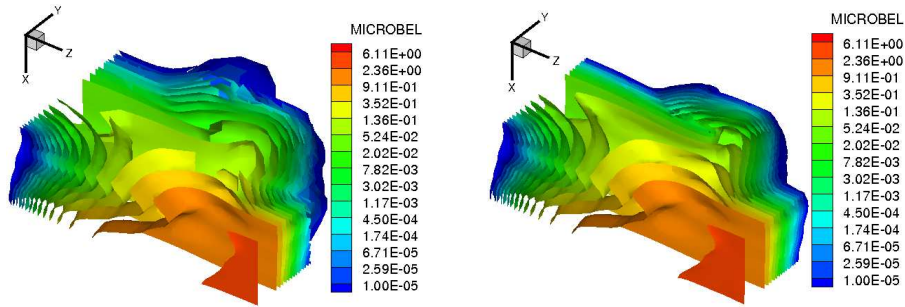


Figure 2. Microbe conc. at $t = 40$ days: multiblock (left) and single block (right).

Then the problem is repeated by partitioning the domain into three sub-domains (one fine and two coarse) along the y - direction. This is done in three different ways by placing the sub-domain with the fine grid differently in each case. The single- and multi- block solutions are then compared. Comparison of the microbe concentrations at time $t = 40$ days for the single-domain and a multiblock case is shown in figure 2. It is noted that the front has crossed $y = 280'(\Gamma_{2,3})$. Similar comparison at $t = 40$ days is shown in figure 3 for the NAPL concentration. It is observed that the spread

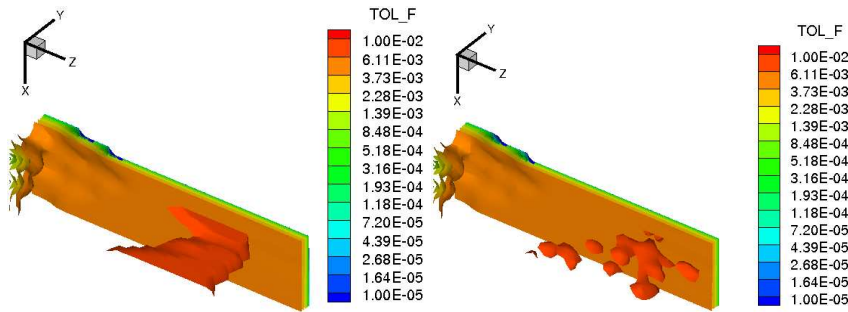


Figure 3. NAPL conc. at $t = 40$ days: multiblock (left) and single block (right).

of NAPL has been checked to some extent by the reaction with the microbes. The microbes “feed” on the NAPL in the presence of O_2 and N_2 , reducing them to relatively harmless by-products. This illustrates the importance of using bio-remediation methods in treating hazardous wastes.

5. Conclusions

In the numerical experiments described, it was observed that variably refined sub-domains (one fine and two coarse with the fine sub-domain located differently in each case) performed up to 50% faster than the single domain “fine-everywhere” case. This justifies the use of mortars in such problems. However, it is noted that coarser sub-domain grid results in increased grid dispersion effects and hence, dynamic meshing strategy is recommended. Further, an implicit-in-time treatment of the interface term in [17] remains to be tested as in [WHE 02].

6. References

- [ARB 97] ARBOGAST T., WHEELER M. F., YOTOV I., “Mixed finite elements for elliptic problems with tensor coefficients as cell-centered finite differences”, *SIAM J. Numer. Anal.*, vol. 34, num. 2, 1997, p. 828–852.
- [BRE 91] BREZZI F., FORTIN M., *Mixed and hybrid finite element methods*, Springer-Verlag, New York, 1991.
- [CHA 84] CHAN T. F., “Stability analysis of finite difference schemes for the advection-diffusion equation”, *SIAM J. Numer. Anal.*, vol. 21, num. 2, 1984, p. 272–284.
- [CHA 86] CHAVENT G., JAFFRE J., *Mathematical models and finite elements for reservoir simulation*, North-Holland, Amsterdam, 1986.
- [CHE 89] CHEN Z., DOUGLAS, JR. J., “Prismatic mixed finite elements for second order elliptic problems”, *Calcolo*, vol. 26, 1989, p. 135–148.
- [CIA 78] CIARLET P. G., *The finite element method for elliptic problems*, North-Holland, Amsterdam, 1978, Studies in Mathematics and its Applications, Vol. 4.
- [NED 80] NEDELEC J. C., “Mixed finite elements in \mathbf{R}^3 ”, *Numer. Math.*, vol. 35, 1980, p. 315–341.
- [PES 01] PESZYNSKA M., SUN S., “Multiphase reactive transport module TRCHEM in IPARSv2”, report num. TICAM01-32, 2001, CSM, University of Texas at Austin, Austin, TX.
- [RAV 77] RAVIART R. A., THOMAS J. M., “A mixed finite element method for 2nd order elliptic problems”, *Mathematical Aspects of the Finite Element Method, Lecture Notes in Mathematics*, vol. 606, p. 292-315, Springer-Verlag, New York, 1977.
- [WHE 02] WHEELER J. A., WHEELER M. F., YOTOV I., “Enhanced velocity mixed finite element methods for flow in multiblock domains”, *Comp. Geo.*, vol. 6, 2002, p. 315–332.
- [YOT 01] YOTOV I., “Interface solvers and preconditioners of domain decomposition type for multiphase flow in multiblock porous media”, *Scientific computing and applications (Kananaskis, AB, 2000)*, vol. 7 of *Adv. Comput. Theory Pract.*, p. 157–167, Nova Sci. Publ., Huntington, NY, 2001.